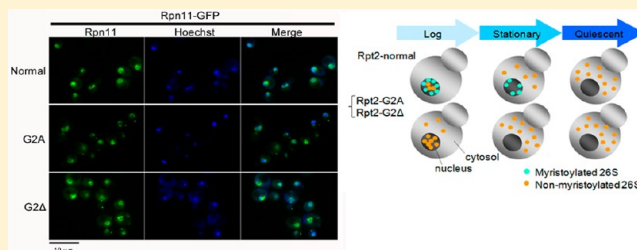


# N-Myristoylation of the Rpt2 Subunit Regulates Intracellular Localization of the Yeast 26S Proteasome

Ayuko Kimura,<sup>†,‡</sup> Yu Kato,<sup>‡</sup> and Hisashi Hirano<sup>\*,†,‡</sup><sup>†</sup>Advanced Medical Research Center, Yokohama City University, Fukuura 3-9, Kanazawa, Yokohama 236-0004, Japan<sup>‡</sup>Department of Supramolecular Biology, Graduate School of Nanobioscience, Yokohama City University, Suehiro 1-7-29, Tsurumi, Yokohama 230-0045, Japan

## S Supporting Information

**ABSTRACT:** The 26S proteasome is a large, complex multisubunit protease involved in protein quality control and other critical processes in eukaryotes. More than 110 post-translational modification (PTM) sites have been identified by a mass spectrometry of the 26S proteasome of *Saccharomyces cerevisiae* and are predicted to be implicated in the dynamic regulation of proteasomal functions. Here, we report that the N-myristoylation of the Rpt2 subunit controls the intracellular localization of the 26S proteasome. While proteasomes were mainly localized in the nucleus in normal cells, mutation of the N-myristoylation site of Rpt2 caused diffusion of the nuclear proteasome into the cytoplasm, where it formed aggregates. In mutant cells, the level of accumulation of cytoplasmic proteasomes was significantly increased in the nonproliferating state. Although the molecular assembly and peptidase activity of the 26S proteasome were totally unchanged in the nonmyristoylated mutants of Rpt2, an increased level of accumulation of polyubiquitinated proteins and a severe growth defect were observed in mutant cells induced for protein misfolding. In addition, polyubiquitinated protein and the nuclear protein Gcn4 tended not to colocalize with the proteasome in normal and mutant cells. Our results suggest that N-myristoylation is involved in regulating the proper intracellular distribution of proteasome activity by controlling the nuclear localization of the 26S proteasome.



The 26S proteasome is a large multisubunit complex involved in proteolysis of polyubiquitin-tagged proteins by the ubiquitin–proteasome system (UPS), a major component in the protein quality control system. Proteins misfolded within the endoplasmic reticulum (ER) are also polyubiquitinated and exported into the cytoplasm for rapid proteasomal degradation in a process called ER-associated degradation (ERAD). In addition, various cellular processes such as the cell cycle and stress responses are under control of the UPS.<sup>1</sup> Tight regulation of proteins' half-lives ensures the expression of their functions at appropriate times and locations within the cell.

The 26S proteasome of eukaryotes is present in both the cytoplasm and nucleus. The functions of cytoplasmic proteasomes have been extensively analyzed; however, a growing body of evidence indicates that the nuclear proteasomes also play critical roles in the control of various nuclear functions such as gene expression, DNA repair, and nuclear protein quality control.<sup>1</sup> Proportions of nuclear to cytoplasmic proteasomes vary, likely depending on the cell types, culture phases, and detection methods.<sup>1–4</sup> The 26S proteasome is synthesized within the cytoplasm and partly imported into the nucleus through the nuclear pore complex,<sup>5,6</sup> whereas the active transport of proteasomes from the nucleus to the cytoplasm has not been observed. In multicellular organisms, the cytoplasmic and nuclear pools of proteasomes are separated by the nuclear envelope. Proteasomes accumulate

within the nucleus during the interphase and are rapidly equilibrated by degradation of the nuclear envelope during mitosis.<sup>7</sup> In yeast, a unicellular organism with closed mitosis, the nuclear envelope proteins Cut8 or Sts1 tether the proteasome on the nuclear envelope, resulting in a predominantly nuclear localization of the proteasome, as has been described by many groups.<sup>8–11</sup> The role of the mammalian homologue of Cut8 and Sts1, which exhibits a low level of sequence similarity to yeast Cut8 and Sts1, remains unclear.<sup>12</sup>

The 26S proteasome consists of the 19S regulatory particle (RP) and the 20S core particle (CP). Polyubiquitinated proteins are captured by the 19S RP lid and transported into the catalytic subunit 20S CP with aid of the 19S ATPase. Thus, the degradation of polyubiquitinated proteins by the 20S CP is controlled not only by the association with the 19S RP but also by the ubiquitin binding activity and ATPase activity of the 19S RP. These activities, as well as the catalytic activity of the 20S CP itself, are predicted to be dynamically controlled by the various post-translational modifications (PTMs), as demonstrated previously in several reports.<sup>13–16</sup> However, there is still little direct evidence regarding the role of the particular PTM site of the proteasome.

Received: June 13, 2012

Revised: October 10, 2012

Published: October 26, 2012



Table 1. Strains and Plasmids Used in This Study

strain	relevant genotype	source
BY4741	<i>MAT a his3-Δ1 leu2-Δ1 ura3-Δ0 met15-Δ1</i>	our stock
BY4741-pRS316	<i>MAT a his3-Δ1 leu2-Δ1 ura3-Δ0 met15-Δ1 pRS316</i>	this study
α4-GFP	<i>MAT a his3-Δ1 leu2-Δ1 ura3-Δ0 met15-Δ1 α4::α4-GFP-hisMX6 RPT2Δ::kanMX6 RPT2/pRS316</i>	this study
rpn11-GFP	<i>MAT a his3-Δ1 leu2-Δ1 ura3-Δ0 met15-Δ1 RPN11::RPN11-GFP-His3MX6 RPT2Δ::kanMX6 RPT2/pRS316</i>	this study
rpn11-TEV-proA	<i>MAT a his3-Δ1 leu2-Δ1 ura3-Δ0 met15-Δ1 RPN11::RPN11-GFP-His3MX6 RPT2Δ::kanMX6 RPT2/pRS316</i>	this study
rpt2-GFP	<i>MAT a his3-Δ1 leu2-Δ1 ura3-Δ0 met15-Δ1 RPN11::RPN11-GFP-His3MX6 RPT2Δ::kanMX6 RPT2-GFP/pRS315</i>	this study
RPT2 (normal) (α4-GFP)	<i>MAT a his3-Δ1 leu2-Δ1 ura3-Δ0 met15-Δ1 α4::α4-GFP-hisMX6 RPT2Δ::kanMX6 RPT2/pRS315</i>	this study
rpt2-G2A (α4-GFP)	<i>MAT a his3-Δ1 leu2-Δ1 ura3-Δ0 met15-Δ1 α4::α4-GFP-His3MX6 RPT2Δ::kanMX6 rpt2(G2A)/pRS315</i>	this study
rpt2-G2Δ (α4-GFP)	<i>MAT a his3-Δ1 leu2-Δ1 ura3-Δ0 met15-Δ1 α4::α4-GFP-His3MX6 RPT2Δ::kanMX6 rpt2(G2Δ)/pRS315</i>	this study
rpt2 (normal) (rpn11-GFP)	<i>MAT a his3-Δ1 leu2-Δ1 ura3-Δ0 met15-Δ1 RPN11::RPN11-GFP-His3MX6 RPT2Δ::kanMX6 RPT2/pRS315</i>	this study
rpt2-G2A (rpn11-GFP)	<i>MAT a his3-Δ1 leu2-Δ1 ura3-Δ0 met15-Δ1 RPN11::RPN11-GFP-His3MX6 RPT2Δ::kanMX6 rpt2(G2A)/pRS315</i>	this study
rpt2-G2Δ (rpn11-GFP)	<i>MAT a his3-Δ1 leu2-Δ1 ura3-Δ0 met15-Δ1 RPN11::RPN11-GFP-His3MX6 RPT2Δ::kanMX6 rpt2(G2Δ)/pRS315</i>	this study
rpt2 (normal) (rpn11-TEV-proA)	<i>MAT a his3-Δ1 leu2-Δ1 ura3-Δ0 met15-Δ1 RPN11::RPN11-TEVproA(HIS3) RPT2Δ::kanMX6 RPT2/pRS315</i>	this study
rpt2-G2A (rpn11-TEV-proA)	<i>MAT a his3-Δ1 leu2-Δ1 ura3-Δ0 met15-Δ1 RPN11::RPN11-TEVproA(HIS3) RPT2Δ::kanMX6 rpt2(G2A)/pRS315</i>	this study
rpt2-G2Δ (rpn11-TEV-proA)	<i>MAT a his3-Δ1 leu2-Δ1 ura3-Δ0 met15-Δ1 RPN11::RPN11-TEVproA(HIS3) RPT2Δ::kanMX6 rpt2(G2Δ)/pRS315</i>	this study
plasmid	composition	source
pBluescript (SK-)	Amp <sup>r</sup>	Agilent Technology
pFA6a-kanMX6	pTEF Kan <sup>r</sup> tTEF	27
pFA6a-His3MX6	pTEF His5 <sup>+</sup> tTEF	27
pFA6a-GFP(S65T)-His3MX6	GFP(S65T) tADH1 His3	27
pRS316	URA3 CEN6 ARSH4	28
pRS315	Leu2 CEN6 ARSH4	28
pAUR123	pADH1 tADH1 Amp <sup>r</sup> CEN4 ARS1 AURI-C	TAKARA
Rpt2-GFP/pRS306	rpt2-GFP in pRS306	this study
RPT2/pRS316	RPT2 in pRS316	this study
RPT2/pRS315	RPT2 in pRS315	this study
rpt2(G2A)/pRS315	rpt2(G2A) in pRS315	this study
rpt2(G2Δ)/pRS315	rpt2(G2Δ) in pRS315	this study
CFP-UBI4/pAUR123	CFP-UBI4 in pAUR123	this study

Previously, we identified more than 110 PTM sites in the 34 subunits of the yeast 26S proteasome using mass spectrometry.<sup>17–20</sup> In comprehensive studies of the N-terminal peptides of the 26S proteasome, we found that the N-termini of 21 subunits are acetylated, while the N-termini of 11 subunits remained unmodified. In addition, we identified one N-myristoylation site, a relatively rare lipid modification, in the Rpt2 subunit.<sup>19</sup> N-Myristoylation of Rpt2 at the Gly<sup>2</sup> residue has also been identified in humans,<sup>21</sup> mice,<sup>22</sup> and rice<sup>23</sup> using mass spectrometry. The glycine residue is extensively conserved in many other eukaryotes, indicating the general importance of this modification. However, the role of the N-myristoylation of Rpt2 remains to be clarified. N-Myristoylation is an irreversible PTM in which myristic acid, a 14-carbon saturated fatty acid, is covalently attached to a glycine residue in a protein's N-terminus. It is widely accepted that N-myristoyl moieties mediate hydrophobic interactions with membrane lipid or other proteins and are involved in the intracellular localization or intermolecular interaction of modified proteins.<sup>24</sup>

Recently, the complete subunit structure of the yeast 19S RP was reported by Lander et al.<sup>25</sup> This structure demonstrates that the N-terminal helices of a pair of neighboring 19S ATPases, Rpt3 with Rpt6 and Rpt4 with Rpt5, form a coiled-coil protrusion, which are predicted to interact with the Rpn2 and Rpn10 subunits, respectively. In contrast, Rpt1 and Rpt2 are unlikely to participate in coiled-coil formation. The N-

terminal α-helix of Rpt1 is likely to interact with the C-terminus of Rpn1, whereas there is currently no information available regarding the structural details and functions of the N-terminus of Rpt2.

To characterize the role of N-myristoylation of the Rpt2 subunit, we analyzed the molecular assembly, activity, and intracellular localization of the 26S proteasome in cells expressing nonmyristoylated mutants of Rpt2. In these mutant strains, the Gly residue at the myristoylation site has been either replaced with Ala (*rpt2-G2A*) or deleted (*rpt2-G2Δ*). A single mutation in the N-myristoylation site of Rpt2 induced the redistribution of proteasomes from the nucleus to the cytoplasm, resulting in the appearance of proteasome aggregates within the cytoplasm. This is the first report demonstrating that the PTM of a single subunit influences the intracellular localization of an entire protein complex without affecting its molecular assembly or activity.

## MATERIALS AND METHODS

**Yeast Strains, Plasmids, and Spot Assays.** Strains and plasmids used in this study are listed in Table 1. All strains were constructed from the BY4741 strain, by inserting the GFP or TEV-protein A tag into the endogenous *RPN11*, *PRE6* (α4), or *RPT2* genes using a polymerase chain reaction (PCR)-based method.<sup>26–28</sup> The TEV-protein A tag, which was used for affinity purification of proteasome,<sup>29</sup> was inserted into the 3'-

end of the coding sequence of the endogenous RPN11 gene using a PCR-based method.<sup>26</sup> The rpn11-GFP and  $\alpha$ 4-GFP strains were constructed by inserting the GFP sequence into the endogenous *RPN11* and  $\alpha$ 4 genes by the same method, using a PCR fragment amplified from the pFA6a-GFP (S65T)-His3MX6 plasmid.<sup>27</sup> Because the deletion of the *RPT2* gene is lethal for yeast, *rpt2*-G2A and *rpt2*-G2 $\Delta$  strains were constructed by plasmid shuffling. The *RPT2* (normal), *rpt2*-G2A, and *rpt2*-G2 $\Delta$  genes with 1 kb of 5' UTR sequence were subcloned into the BamHI and XhoI sites of the pRS315 or pRS316 vector.<sup>28</sup> The *RPT2*/pRS316 plasmid was transformed into the rpn11-GFP,  $\alpha$ 4-GFP, and rpn11-TEV-proA strains, and the *rpt2*-GFP/pRS316 plasmid was transformed into the rpn11-TEV-proA strain. The endogenous *RPT2* gene was substituted using the pFA6a-His3MX6 cassette<sup>27</sup> by homologous recombination, and positive clones were selected on SC-URA/His plates. The growth of cells was checked by the spot assay on SC-URA plates at 30 and 37 °C. Then, the *RPT2*/pRS315, *rpt2*-G2A/pRS315, and *rpt2*-G2 $\Delta$ /pRS315 plasmids were transformed, and clones were selected on SC-URA/Leu plates. Plasmid shuffling was performed on SC-Leu/5'-FOA plates. For two-color imaging, a cDNA fragment containing the open reading frame of the *Saccharomyces cerevisiae* *UBI4* gene, N-terminally tagged with CFP, was cloned into the pAUR123 vector (Takara). The resulting vector was transformed into rpn11-GFP strains.

For the spot assay, cells precultured on SC-Leu plates were diluted to an OD<sub>600</sub> of 1, spotted onto SC-Leu (or SC-Leu/Arg for canavanine) plates supplemented with the indicated reagents, and incubated for 3–5 days at 30 °C unless specified otherwise.

**Sodium Dodecyl Sulfate–Polyacrylamide Gel Electrophoresis (SDS–PAGE) of Yeast Cell Lysates and Immunoblot Assay.** Whole cell lysates were extracted from rpn11-TEV-proA strains by vortexing with glass beads in lysis buffer [20 mM HEPES (pH 8.0) and 9 M urea]. Polyubiquitinated proteins were detected by immunoblotting, using antibodies against mono- and polyubiquitinated conjugates (FK2H) (Enzo Life Sciences). Proteasome subunits  $\alpha$ 4 (20S) and Rpn11 (19S) were detected in the same lysates using antibodies against anti-PSMA7 ( $\alpha$ 4) (AP8659c, Abgent) and the peroxidase–antiperoxidase (PAP) soluble complex (Sigma).

**Native PAGE of Yeast Cell Lysates, In-Gel Peptidase Assay, and Immunoblot Assay.** Stationary cultures grown in SC-Leu medium at 30 and 37 °C were lysed by vortexing with glass beads in native lysis buffer [50 mM Tris-HCl (pH 7.5), 2 mM ATP, 5 mM MgCl<sub>2</sub>, 1 mM DTT, and 1.5% (v/v) glycerol], supplemented with protease inhibitor cocktail and phosphatase inhibitor cocktail (Nacalai Tesque). After centrifugation, 30  $\mu$ g of cleared lysate was loaded onto 4% native polyacrylamide gels with 0.45 mM Tris-Boric acid buffer (pH 8.3), 5 mM MgCl<sub>2</sub>, 2 mM ATP, 0.5 mM EDTA, and 1 mM DTT. Electrophoresis was performed at 4 °C for 2 h at 100 V. Gels were washed in developing buffer [50 mM Tris-HCl (pH 7.4), 5 mM MgCl<sub>2</sub>, and 1 mM ATP] and incubated in developing buffer containing 50  $\mu$ M succinyl-Leu-Leu-Val-Tyr 4-methyl-coumaryl-7-amide [Suc-LLVY-MCA (Peptide Institute, Osaka, Japan)] for 30 min at 30 °C. Signals were detected using an ImageQuant LAS 4000-mini biomolecular imager equipped with a UV filter. Proteins in native PAGE gels were blotted onto PVDF membranes after the gels had been soaked in 1 $\times$  SDS sample

buffer and transfer buffer. The 26S proteasome was detected using the anti- $\alpha$ 4 antibody.

**Purification of Proteasomes, Mass Spectrometry, and Peptidase Assay.** The 26S proteasome was purified from the cells expressing Rpn11-TEV-ProA as described by Kikuchi et al.,<sup>18</sup> using cells grown in SC-Leu medium for 72 h at 30 °C. The purified 26S proteasome was separated on a 3 to 10% gradient gel (Wako) and stained with Coomassie Brilliant Blue R-250. Each band was excised from the gel, and in-gel trypsin digestion was performed overnight at 37 °C. Peptide solutions were analyzed using MALDI-TOF/TOF-MS (4800, AB Sciex) and LC-LTQ Orbitrap (Thermo Scientific) and identified using MASCOT (Matrix Science). For peptidase assays, 2  $\mu$ g of the purified proteasome was incubated with 100  $\mu$ M Suc-LLVY-AMC, Ac-DEVD-MCA, or Boc-LRR-MCA (Peptide Institute) in reaction buffer [50 mM Tris-HCl (pH 7.5), 40 mM KCl, 5 mM MgCl<sub>2</sub>, 0.5 mM ATP, 1 mM DTT, and 50  $\mu$ g/mL BSA] at room temperature. Fluorescent signals were detected using an Infinite F200 multimode microplate reader (Tecan) equipped with a 340 nm excitation filter and a 465 nm emission filter.

**Fluorescence Microscopy.** Yeast cells were grown at 30 or 37 °C in 10 mL of SC-Leu medium for 5 h (log), 24 h (stationary), or 1 week (quiescent), harvested by centrifugation, and stained with 5  $\mu$ L of the DNA staining dye Hoechst 33342 (Dojindo). GFP and Hoechst signals were detected in unfixed cells, using a fluorescence microscope (BZ-9000, Keyence) equipped with fluorescence filters for GFP and DAPI and a Plan Apo 100 $\times$ , 1.40 oil objective lens (Nikon). ER was stained with ER stain (Subcellular Structure Localization Kit, Chemicon) and detected using a fluorescence filter appropriate for GFP. For the detection of actin, yeast cells were fixed in 4% (v/v) formaldehyde for 30 min and incubated with rhodamine-phalloidin (Subcellular Structure Localization Kit) for 2 h; these samples were observed using fluorescence filters appropriate for TRITC. For counting cells containing dotlike signals, images were obtained by overlapping the z-stack images collected at a step size of 0.2  $\mu$ m. Canavanine-treated cells were streaked on SC-Leu plates with 2  $\mu$ g/mL canavanine, cultured for 3 days, and harvested for observation. Quantification of the fluorescence intensity of each pixel was performed using the BZ-II image analysis application (Keyence). Photobleaching was conducted using a Zeiss LSM510 confocal microscope equipped with a C-Apochromat 63 $\times$ , 1.2 Corr objective lens. A 30 mW argon laser was turned on at 75% power. For fluorescence recovery after photobleaching (FRAP) experiments, 10 iterative laser pulses at full power were applied to the nucleus or cytoplasm of the rpn11-GFP strains, and three images were collected at 30 min intervals.

**Cell Fractionation.** Yeast cells were grown for 24 h at 30 °C in 1 L of SC-Leu medium. The cell pellet was collected by centrifugation, and the supernatant was reused to make SC-Leu/S (2 M sorbitol in SC-Leu) medium, to avoid changing the localization pattern of the proteasome. The cell pellet was resuspended in 50 mM Tris-HCl (pH 7.5) and 30 mM DTT and incubated for 30 min at 30 °C. After centrifugation, cells were resuspended in SC-Leu/S and spheroplasted by incubation with 10 mg/mL Zymolyase 20T for 1 h at 30 °C. The pellet was resuspended and incubated for 30 min in SC-Leu/S at 30 °C and then washed twice with ice-cold SC-Leu/S and once with ice-cold 1 M sorbitol. Cells were resuspended in 6 mL of ice-cold buffer A [10 mM Tris (pH 7.5), 18% Ficoll, 20 mM potassium acetate, 5 mM magnesium acetate, 1 mM EDTA, 3 mM DTT, and protease inhibitor cocktail] and lysed



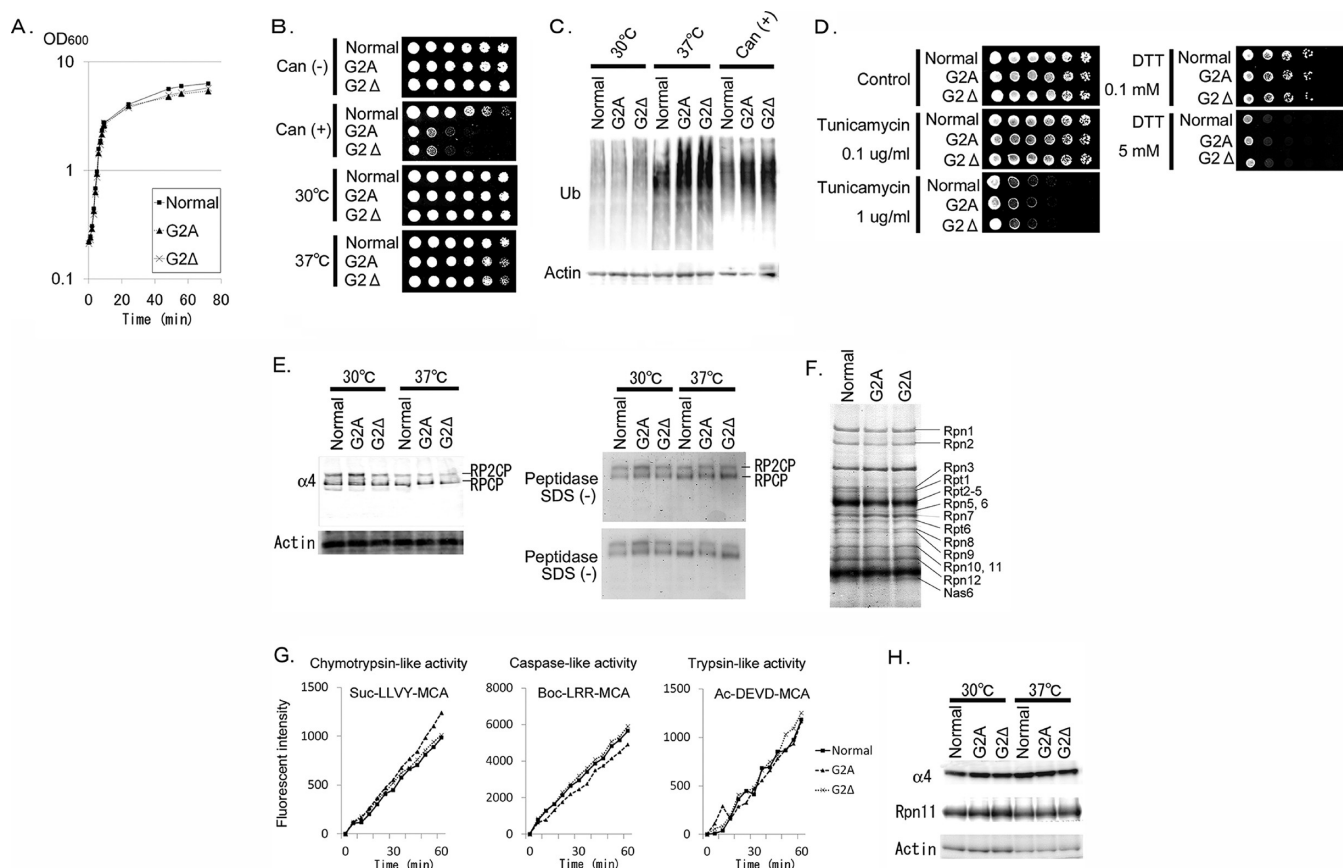


**Figure 1.** Phenotypes of *RPT2*, *rpt2*-G2A, and *rpt2*-G2Δ cells. (A) Growth curve. OD<sub>600</sub> values of *RPT2*, *rpt2*-G2A, and *rpt2*-G2Δ cells at each time point are shown on a semilogarithmic graph. (B) Spot assay under normal and restrictive conditions. Dilutions of Rpn11-TEV-proA cells (4-fold) expressing Rpt2, Rpt2-G2A, or Rpt2-G2Δ were spotted onto SC-Leu/Arg plates with or without 2 μg/mL canavanine and incubated at 30 °C (top panels). Dilutions of the same cells (10-fold) were spotted onto SC-Leu plates and incubated at 30 or 37 °C (bottom panels). (C) Accumulation of polyubiquitinated proteins under normal or restrictive conditions. The *RPT2*, *rpt2*-G2A, and *rpt2*-G2Δ cells were cultured overnight under the indicated conditions. A total of 10 μg of yeast cell lysate was separated by SDS–PAGE and subjected to an immunoblot assay using the anti-ubiquitin antibody and anti-actin-1 antibody as a loading control. (D) Spot assay under ER stress conditions. Dilutions of cells (4-fold) were spotted onto SC-Leu plates with the indicated dilutions of tunicamycin or DTT. (E) Native PAGE of yeast cell lysate. The lysate was prepared from *RPT2*, *rpt2*-G2A, and *rpt2*-G2Δ cells grown overnight at 30 or 37 °C. A total of 30 μg of native cell lysate was subjected to native PAGE using a 4% polyacrylamide gel. The 26S proteasome was detected both by immunoblotting using the anti-α4 (20S) antibody (top left) and by the in-gel peptidase assay using suc-LLVY-AMC (right). Loaded proteins were also quantified using the anti-actin antibody (SDS–PAGE, bottom left). (F) Pull-down assay. A total of 10 μg of the purified proteasome was analyzed by SDS–PAGE and visualized using CBB staining. Each band was subjected to in-gel MS analysis. 19S subunits identified by MS/MS analysis are indicated. (G) Peptidase assay. Three peptidase activities of the proteasome (chymotrypsin-like, trypsin-like, and caspase-like activities) were analyzed using 2 μg each of proteasomes purified from *RPT2*, *rpt2*-G2A, and *rpt2*-G2Δ cells. (H) SDS–PAGE of yeast cell lysates. A total of 10 μg of lysate, prepared as described for panel C, was subjected to SDS–PAGE; α4 (20S) and Rpn11 (19S) were detected by immunoblot assays.

on ice in a Dounce homogenizer with 20 strokes of the loose pestle and 15 strokes of the tight pestle. Crude nuclei were isolated by centrifugation twice at 3500g for 10 min and twice at 2400g for 5 min. Nuclei were precipitated by centrifugation at 21600g, and the supernatant was collected as the cytoplasmic fraction. Fractionation was confirmed by an immunoblot assay using anti-Hsp70 (61607, BD Transduction Laboratories) and anti-Nop1 (28F2, Santa Cruz Biotechnology) antibodies, which detect cytoplasmic and nuclear markers, respectively. The 20S proteasome and Gcn4 were detected using anti-α4 and anti-Gcn4 (FL-281, Santa Cruz Biotechnology) antibodies, respectively.

## RESULTS

**Growth and Polyubiquitin Accumulation of *rpt2*-G2A and *rpt2*-G2Δ Mutants.** Cells expressing the nonmyristoylated mutants of Rpt2, *rpt2*-G2A and *rpt2*-G2Δ, grew normally

under optimal growth conditions (SC-Leu at 30 °C) (Figure 1A,B). The doubling times of normal (*RPT2*), *rpt2*-G2A, and *rpt2*-G2Δ cells were 2.09, 2.23, and 2.19 h, respectively, with a slight increase in *rpt2* mutant cells (Figure 1A). Both *rpt2*-G2A and *rpt2*-G2Δ mutants exhibited phenotypes indicating decreased proteasome activity: significant sensitivity against canavanine, an arginine analogue, and restricted growth at an elevated temperature (37 °C) (Figure 1B). Under these conditions, polyubiquitinated proteins were present at significantly higher levels in cell lysates from *rpt2*-G2A and *rpt2*-G2Δ cells than those from *RPT2* cells (Figure 1C). To confirm whether the accumulation of polyubiquitinated proteins was caused by a deficiency in ERAD, we also analyzed the effect of tunicamycin and DTT, inducers of ER stress (Figure 1D). The *rpt2*-G2A and *rpt2*-G2Δ cells exhibited no detectable ERAD deficiency, as determined by drug sensitivity.

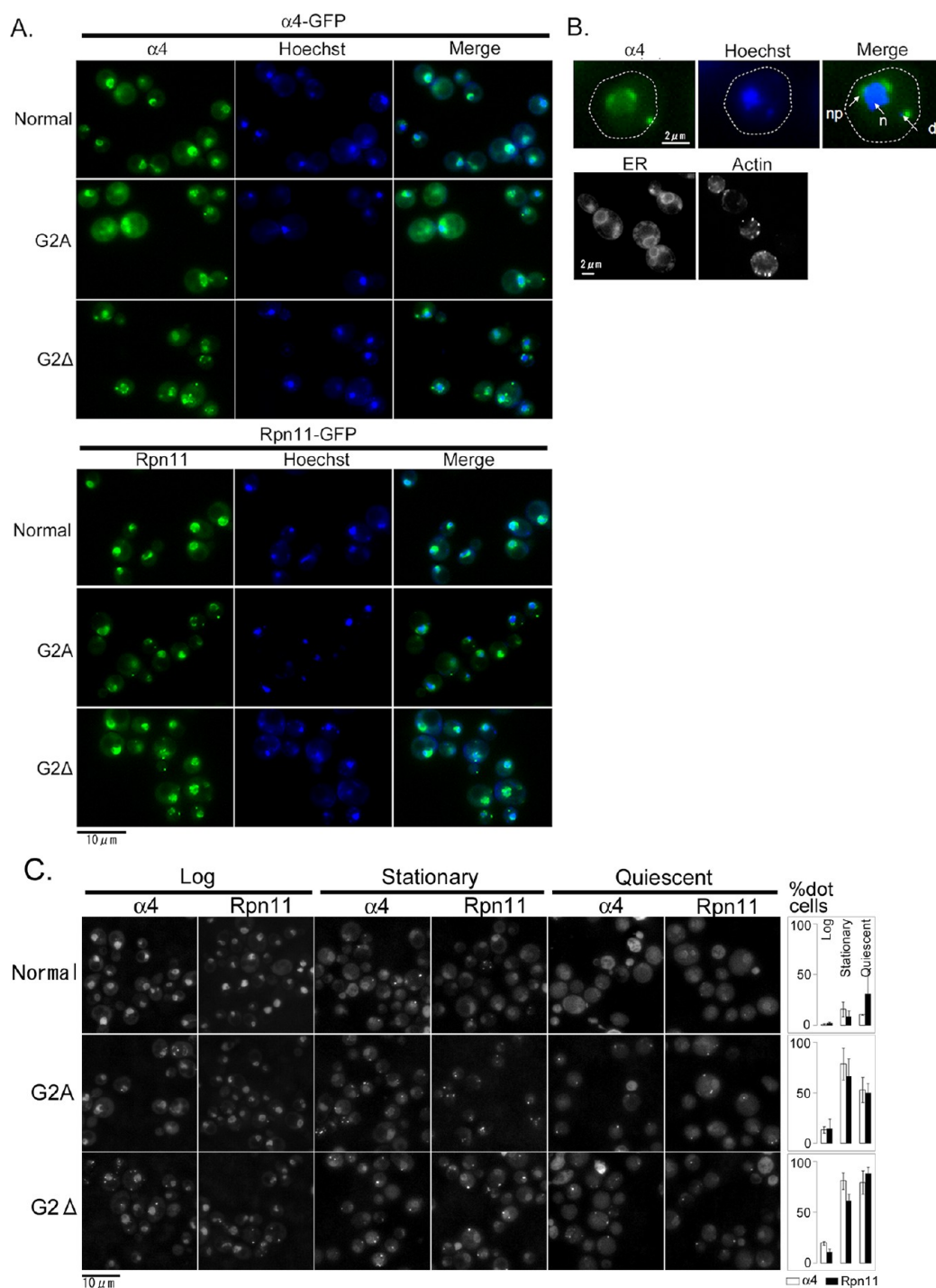


**Figure 2.** Intracellular localization of 26S proteasomes in *RPT2*, *rpt2*-G2A, and *rpt2*-G2 $\Delta$  cells. (A) Intracellular localization of the  $\alpha 4$  and Rpn11 subunits at log phase.  $\alpha 4$ -GFP or Rpn11-GFP was detected after incubation at 30 °C for 5 h. Typical images of the GFP and Hoechst (DNA) signals are shown. (B) Close-up of Hoechst, ER, and actin staining of the representative *rpt2*-G2A cell. Abbreviations: n, nucleus; np, nuclear periphery; d, dot. (C) Time course localization of the  $\alpha 4$  and Rpn11 subunits. Cells cultured for 5 h (log), 1 day (stationary), or 1 week (quiescent) were used. Numbers of cells with more than one dot were counted (right graph).  $n > 200$  cells for each time point (two experiments); error bars show the standard deviation.

**Molecular Assembly and Peptidase Activity of the 26S Proteasome in *rpt2*-G2A and *rpt2*-G2 $\Delta$  Mutants.** To detect the role of N-myristoylation in the molecular assembly of the 26S proteasome, lysates of *RPT2*, *rpt2*-G2A, and *rpt2*-G2 $\Delta$  cells were subjected to native PAGE followed by immunoblot detection of the 20S CP using an anti- $\alpha 4$  antibody

(Figure 1E). The levels of 26S proteasomes, consisting of Rp<sub>2</sub>CP and RpCP, were comparable in all strains incubated at 30 and 37 °C. The detailed subunit composition of the 19S RP was also confirmed by affinity purification of proteasomes using the TEV-proA tag inserted into the endogenous Rpn11 subunit. The SDS-PAGE pattern of the purified 19S RP was similar

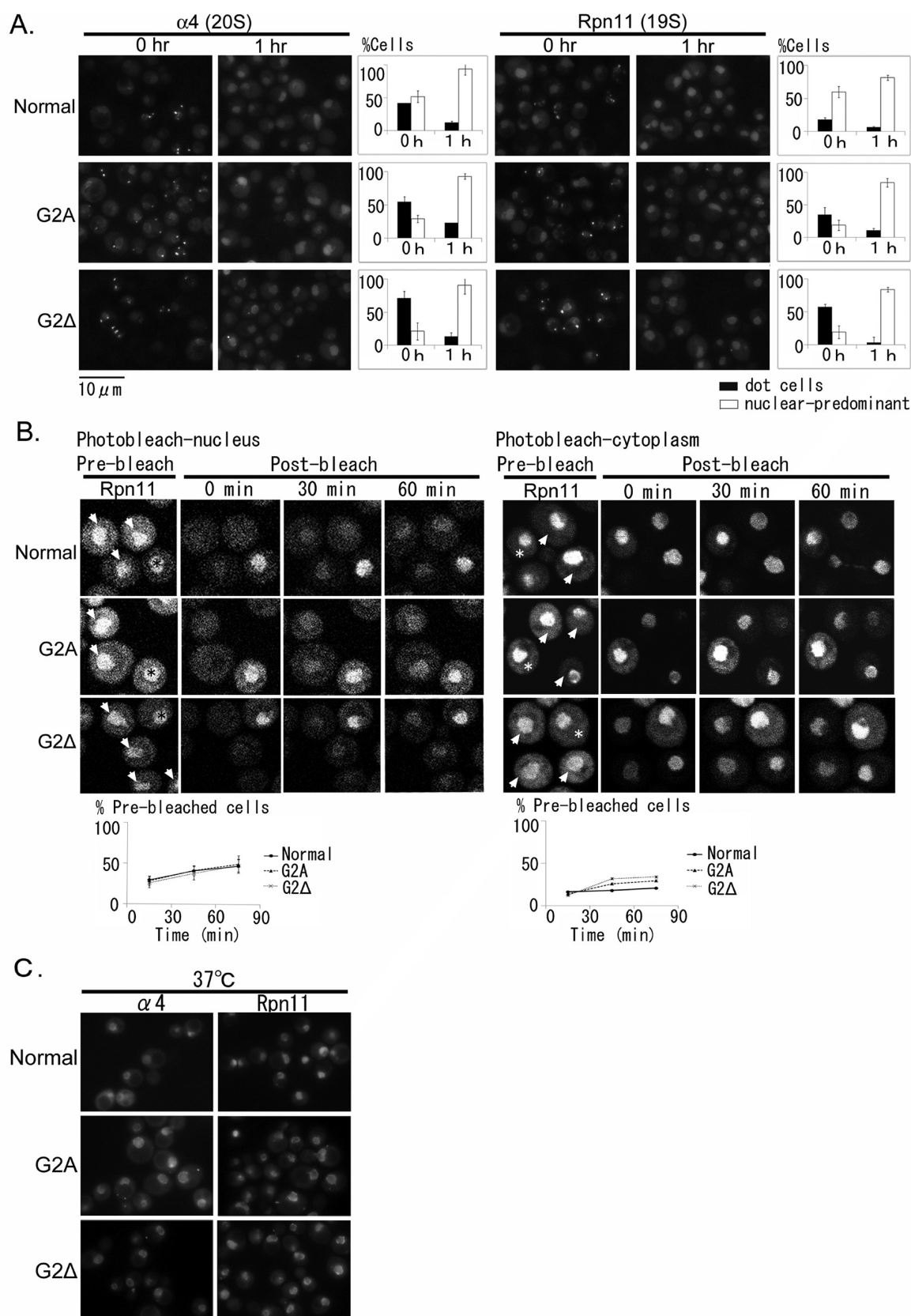


**Figure 3.** Intracellular localization of 26S proteasomes after medium exchange, photobleaching, or incubation at the restrictive temperature. (A) Recovery of the nuclear proteasome by medium exchange. Recovery of signals was observed in culture 0 or 1 h after the transfer of stationary phase cells into new media to induce exit from the quiescent phase.  $n > 200$  cells for each time point (two experiments); error bars show the standard deviation. (B) Recovery of the nuclear and cytoplasmic proteasome after photobleaching. Using logarithmically growing *rpn11*-GFP cells, nuclear import of the proteasome was detected by photobleaching of the entire nucleus (left), whereas nuclear export of the proteasome was detected by photobleaching of the entire cytoplasm (right). Bleached cells are denoted with white arrows, and unbleached cells (controls) are denoted with

Figure 3. continued

asterisks. The relative signal intensity of postbleached to prebleached nucleus and cytoplasm is plotted on the graph below. (C) Intracellular localization of the 26S proteasome at the restrictive temperature. Stationary phase cultures incubated at the restrictive temperature (37 °C) were observed.

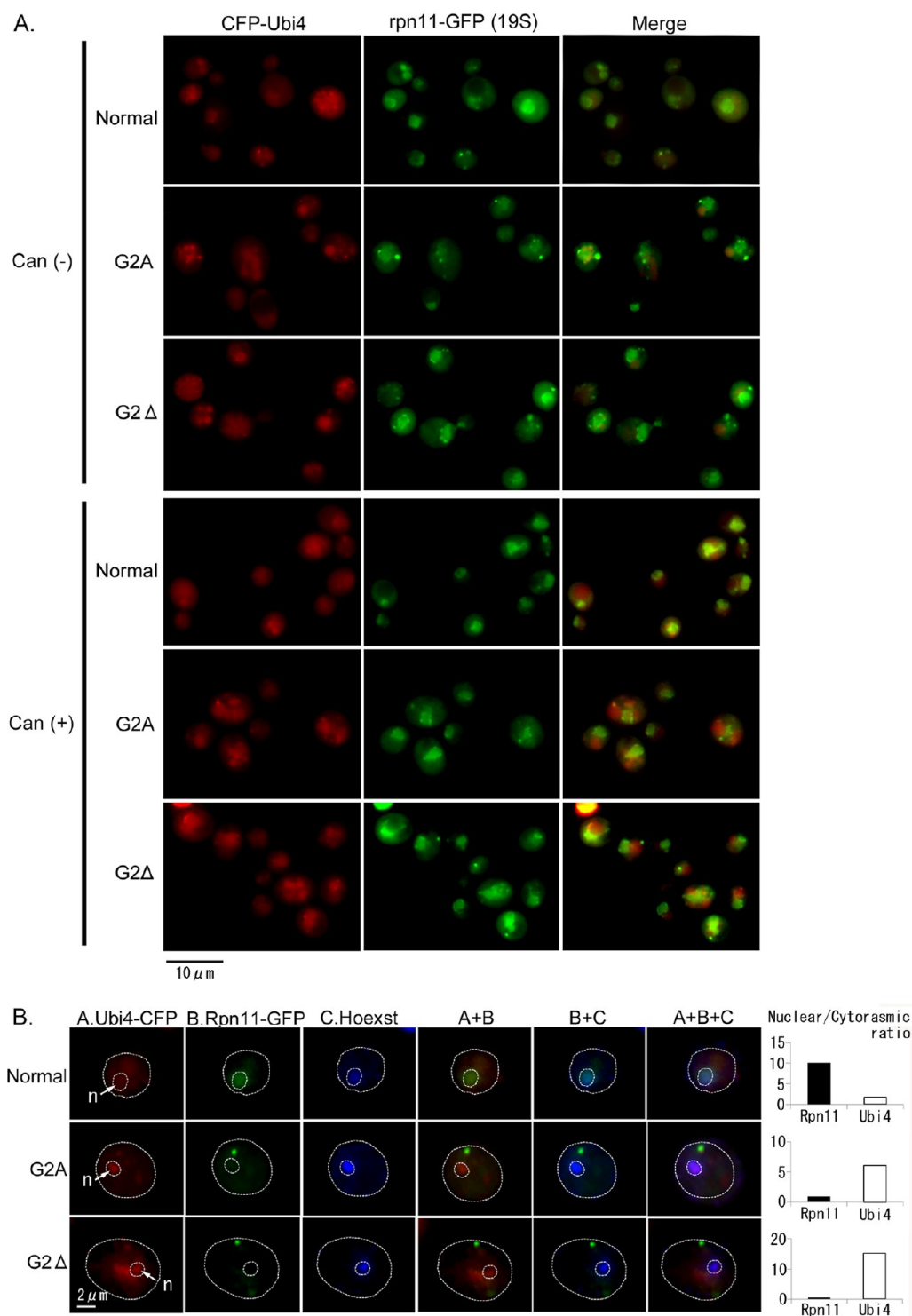


**Figure 4.** Intracellular localization of the polyubiquitin protein Ubi4 in *RPT2*, *rpt2-G2A*, and *rpt2-G2Δ* cells after canavanine treatment. (A) Two-color fluorescent imaging of CFP-Ubi4 (red) and Rpn11-GFP (green). Cells incubated on SC-Leu/aureobasidine plates with or without canavanine were visualized. (B) Close-up of the intracellular localization of the CFP-Ubi4 (red), Rpn11-GFP (green), and Hoechst (blue) signals in *RPT2*, *rpt2-G2A*, and *rpt2-G2Δ* cells. Cells incubated on SC-Leu/aureobasidine plates containing canavanine and stained with Hoechst 33342 were visualized. The relative signal intensity of the nucleus to cytoplasm is plotted in the graph. Nuclei are denoted with white arrows.



between *RPT2* and *rpt2* mutant cells (Figure 1F). Consistent with the data obtained by Kimura et al.,<sup>19</sup> both the N-myristoylated and nonmyristoylated form of Rpt2 could be detected in *RPT2* cells (Figure S1A,B of the Supporting Information). In *rpt2*-G2A and *rpt2*-G2Δ mutants, the modification of the N-terminus of Rpt2 was replaced by acetylation, a ubiquitous N-terminal modification in the 26S proteasome (Figure S1C,D of the Supporting Information).

The peptidase activity of the native 26S proteasome was analyzed by an in-gel peptidase assay using the native PAGE gels, prepared as indicated above. The chymotryptic activity of the 26S proteasome was similar between *RPT2* and *rpt2* mutant cells (Figure 1E). It has been previously reported that the deletion of three amino acid residues from the C-terminus of Rpt2 decreases the peptidase activity of the 26S proteasome, but that this activity is recovered upon treatment with 0.02% SDS (Figure 1E), which causes an artificial opening of the gate of the 20S CP.<sup>30</sup> In our experiment, mutation of the N-myristoylation site of Rpt2 did not change its peptidase activity regardless of the presence or absence of 0.02% SDS, indicating that the gating activity of 19S ATPase was not affected by these mutations. The chymotrypsin-like, trypsin-like, and caspase-like activities of the proteasomes purified from each strain were also comparable between the *RPT2* and *rpt2* mutant cells (Figure 1G). Finally, by immunoblot analysis of lysates prepared under denaturing conditions (9 M urea) (Figure 1H), we confirmed that the total proteasome levels were equal among these strains. Thus, we excluded the possibility that deficiencies in proteasome assembly and activity were masked by the overexpression of the proteasome, thereby compensating for the loss of functional proteasomes in mutant cells. These results indicate that the N-myristoylation of the Rpt2 subunit is not involved in the regulation of the assembly or activity of the 26S proteasome.

**Intracellular Localization of the 26S Proteasome in *rpt2*-G2A and *rpt2*-G2Δ Mutants.** Because the formation of the active 26S proteasome occurred normally in *rpt2*-G2A and *rpt2*-G2Δ cells, we hypothesized that N-myristoylation is involved in the regulation of its intracellular localization. To observe the in vivo localization of the 26S proteasome in the living yeast cells, we fused a GFP tag to the endogenous Rpn11 (19S) or α4 (20S) subunits (Figure S2A of the Supporting Information). Cells constitutively expressing Rpt2-GFP were not used because of their significant growth defect under optimal growth conditions (Figure S2B of the Supporting Information). In all cells, the localization patterns of α4 and Rpn11 were similar (Figure 2A), implying that the 26S complex is the predominant form of the proteasome in both *RPT2* and *rpt2* mutant cells as was also indicated in Figure 1E. Upon mutation of the N-myristoylation site of Rpt2, the localization patterns of α4-GFP and Rpn11-GFP were clearly and dramatically altered. Consistent with previous reports,<sup>8–11</sup> both subunits were detected mainly in the nucleus in *RPT2* cells at log phase (Figure 2A). On the other hand, in *rpt2*-G2A and *rpt2*-G2Δ mutants under the same conditions, signals in the nucleus were weakened, and bright dotlike signals appeared in the cytoplasm, showing the shift of proteasome localization from the nucleus to the cytoplasm. In some cells, the signal inside the nucleus had disappeared, whereas signals at the edge of the nucleus were retained (Figure 2B). Dotlike signals within the cytoplasm did not colocalize with mitochondria (Hoechst staining), ER, or actin (Figure 2B). In the stationary phase, dotlike signals for α4 and Rpn11 in the cytoplasm were also

observed in *RPT2* cells, although they were much more prevalent in *rpt2*-G2A and *rpt2*-G2Δ mutants (Figure 2C). The number of cells with dotlike signals did not change in the stationary and quiescent ( $G_0$ ) phase; however, in the quiescent phase, most signals were diffused within the cytoplasm in both *RPT2* and *rpt2* mutant cells (Figure 2C). By contrast, when *RPT2* and *rpt2*-G2A/*rpt2*-G2Δ cells were transferred to fresh medium, there was a decrease in the number of proteasome aggregates in the cytoplasm and a concomitant increase in the signal intensity of proteasomes in the nucleus, as reported by Laporte et al.<sup>8</sup> (Figure 3A). We also measured the nuclear import and export of proteasomes during the log phase by photobleaching the entire nuclei or cytoplasm of cells (Figure 3B). The rates of recovery of nuclear signals following photobleaching of nuclei were comparable between *RPT2* and *rpt2*-G2A/*rpt2*-G2Δ cells. In contrast, after the cytoplasm had been photobleached, signals recovered faster in *rpt2*-G2A/*rpt2*-G2Δ cells than in *RPT2* cells. Nuclear export was relatively slow compared to nuclear import, as has also been reported in *Schizosaccharomyces pombe*.<sup>31</sup> Taken together, these data indicate that N-myristoylation likely inhibits the leakage of nuclear proteasomes into the cytoplasm but is not involved in proteasome import.

As indicated above, the unique localization pattern of the 26S proteasome of *rpt2*-G2A and *rpt2*-G2Δ mutants was observed under normal conditions without any stress or induction of protein misfolding. Incubation of *RPT2*, *rpt2*-G2A, and *rpt2*-G2Δ cells at the restrictive temperature (37 °C) or in the presence of canavanine caused no significant changes in the localization pattern of the proteasome as compared to that of untreated cells (Figures 3C and 4A). To further confirm that the formation of proteasome aggregates is not induced by the accumulation of polyubiquitinated proteins within the cytoplasm, we ectopically expressed a CFP-tagged Ubi4 gene, which encodes a polyubiquitin protein, in the Rpn11-GFP cells, and marked sites in the cell where high levels of polyubiquitinated proteins accumulate. The CFP tag was fused at the N-terminus of the Ubi4 protein, because GFP-Ubi4 is functionally incorporated into polyubiquitin chains in HeLa cells, exhibiting localization patterns similar to those of endogenous polyubiquitin.<sup>32</sup> After canavanine treatment, we observed an increased level of accumulation of CFP-Ubi4 signals in large vesicle-like bodies, predominantly in the cytoplasm but also in the nucleus (Figure 4A,B). The signals for CFP-Ubi4 and Rpn11-GFP tended not to colocalize. Taken together, these data indicate that the unique localization pattern of the proteasome in cells expressing the nonmyristoylated mutant of Rpt2 was not induced by abnormal aggregation of polyubiquitinated proteins. In addition, in some *rpt2*-G2A/*rpt2*-G2Δ cells with a decreased level of the proteasome in the nucleus, the CFP-Ubi4 signals accumulated to a much greater extent in the nucleus (Figure 4B), implying that nuclear localization of the proteasome is involved in the degradation of polyubiquitinated proteins within the nucleus.

Finally, we performed cell fractionation and immunoblot assays to confirm the intracellular distribution of the 20S proteasome and the nuclear protein Gcn4, a transcriptional activator whose expression level is tightly regulated by controlled proteolysis by the proteasome (Figure 5). Efficient separation of the nuclear and cytoplasmic fractions was confirmed by immunoblot analysis using antibodies against Nop1 (nucleolar protein) and Hsp70 (cytoplasmic protein). The magnitude of the signal for α4 (20S) in the nuclear





Sts1, and N-myristoylated Rpt2 are likely involved in independent mechanisms for nuclear localization of the proteasome, because the *sts1-2* (C194Y) mutant exhibited phenotypes different from that of the *rpt2-G2A/rpt2-G2Δ* mutants, diffused cytoplasmic proteasome signals with no detectable aggregation, which was observed only in cells incubated at the restrictive temperature.<sup>35</sup>

A gradual shift of proteasome localization from the nucleus to the cytoplasm has been previously reported in both yeast and human cell lines under conditions of overgrowth or nutritional depletion.<sup>4,8</sup> Our results suggest that N-myristoylation might play a role in inhibiting leakage of the modified 26S proteasome from the nucleus (Figures 3B and 6B). The yeast N-myristoyltransferase is active only in the log phase,<sup>36</sup> indicating that levels of N-myristoylated Rpt2 synthesized during the log phase would slowly decrease from the stationary to the quiescent phase, because the half-life of the 26S proteasome is approximately 12–15 days.<sup>37</sup> In agreement with this speculation, our previous 2-DE/MS analysis revealed that only half of the 26S proteasome is N-myristoylated in the stationary phase culture.<sup>19</sup> Therefore, we conclude that the proper distribution of proteasomes in each phase is controlled by growth phase-dependent fluctuation of the N-myristoyltransferase activity in each cell. The varying localization patterns of the 26S proteasome observed among individual RPT2 cells in the same culture might reflect heterogeneity of the growth phase and N-myristoyltransferase activity.

Mutation of the N-myristoylation site of Rpt2 is likely not to affect the clearance of misfolded proteins within the cytoplasm (Figure 4A). Rather, it might affect the proteasomal degradation of the minor fraction of polyubiquitinated proteins that are localized within the nucleus, as indicated in Figure 4B. The nuclear protein quality control system has been suggested to prevent the formation of insoluble protein aggregates within the nucleus under severe conditions (e.g., heat shock),<sup>38</sup> which might prevent normal cell growth. Accumulation of functionally critical and short-lived proteins within the nucleus, such as proteins involved in the cell cycle or gene expression [e.g., Gcn4 (Figure 5)], might have a much stronger effect on the growth of *rpt2-G2A* and *rpt2-G2Δ* cells, even if the total amount of polyubiquitinated protein is not significantly increased (Figures 1C and 5). Taken together, our results indicate that the N-myristoylation of Rpt2 is involved in the proper distribution of proteasome activity by controlling the intracellular localization of the 26S proteasome.

## ■ ASSOCIATED CONTENT

### ■ Supporting Information

Two figures. This material is available free of charge via the Internet at <http://pubs.acs.org>.

## ■ AUTHOR INFORMATION

### Corresponding Author

\*Telephone: 81-45-787-2791. E-mail: [hirano@yokohama-cu.ac.jp](mailto:hirano@yokohama-cu.ac.jp).

### Funding

This work was partially supported by Special Coordination Fund for Promoting Science and Technology 'Creation and Innovation Centers for Advanced Interdisciplinary'.

### Notes

The authors declare no competing financial interest.

## ■ ACKNOWLEDGMENTS

We thank Koji Kasahara, Ken-ichi Ogura, and Nobuyuki Endo for the technical assistance with the fluorescence microscope and Kazuhiro Ogata, Masaaki Shiina, Noriaki Arakawa, Yayoi Kimura, and Hiroshi Kawasaki for useful discussions.

## ■ ABBREVIATIONS

PTM, post-translational modification; UPS, ubiquitin–proteasome system; ER, endoplasmic reticulum; ERAD, ER-associated degradation; RP, regulatory particle; CP, core particle; PANs, proteasome-activating nucleotidases; PAGE, polyacrylamide gel electrophoresis.

## ■ REFERENCES

- (1) von Mikecz, A. (2006) The nuclear ubiquitin-proteasome system. *J. Cell Sci.* 119, 1977–1984.
- (2) Wojcik, C., and DeMartino, G. N. (2003) Intracellular localization of proteasomes. *Int. J. Biochem. Cell Biol.* 35, 579–589.
- (3) Rivett, A. J., Palmer, A., and Knecht, E. (1992) Electron microscopic localization of the multicatalytic proteinase complex in rat liver and in cultured cells. *J. Histochem. Cytochem.* 40, 1165–1172.
- (4) Machiels, B. M., Henfling, M. E., Broers, J. L., Hendil, K. B., and Ramaekers, F. C. (1995) Changes in immunocytochemical detectability of proteasome epitopes depending on cell growth and fixation conditions of lung cancer cell lines. *Eur. J. Cell Biol.* 66, 282–292.
- (5) Nederlof, P. M., Wang, H. R., and Baumeister, W. (1995) Nuclear localization signals of human and *Thermoplasma* proteasomal  $\alpha$  subunits are functional in vitro. *Proc. Natl. Acad. Sci. U.S.A.* 92, 12060–12064.
- (6) Wendler, P., Lehmann, A., Janek, K., Baumgart, S., and Enenkel, C. (2004) The bipartite nuclear localization sequence of Rpn2 is required for nuclear import of proteasomal base complexes via karyopherin  $\alpha\beta$  and proteasome functions. *J. Biol. Chem.* 279, 37751–37762.
- (7) Reits, E. A., Benham, A. M., Plougastel, B., Neefjes, J., and Trowsdale, J. (1997) Dynamics of proteasome distribution in living cells. *EMBO J.* 16, 6087–6094.
- (8) Laporte, D., Salin, B., Daignan-Fornier, B., and Sagot, I. (2008) Reversible cytoplasmic localization of the proteasome in quiescent yeast cells. *J. Cell Biol.* 181, 737–745.
- (9) Wilkinson, C. R., Wallace, M., Morphew, M., Perry, P., Allshire, R., Javerzat, J. P., McIntosh, J. R., and Gordon, C. (1998) Localization of the 26S proteasome during mitosis and meiosis in fission yeast. *EMBO J.* 17, 6465–6476.
- (10) Enenkel, C., Lehmann, A., and Kloetzel, P. M. (1999) GFP-labelling of 26S proteasomes in living yeast: Insight into proteasomal functions at the nuclear envelope/rough ER. *Mol. Biol. Rep.* 26, 131–135.
- (11) Russell, S. J., Steger, K. A., and Johnston, S. A. (1999) Subcellular localization, stoichiometry, and protein levels of 26 S proteasome subunits in yeast. *J. Biol. Chem.* 274, 21943–21952.
- (12) Takeda, K., Tonthat, N. K., Glover, T., Xu, W., Koonin, E. V., Yanagida, M., and Schumacher, M. A. (2011) Implications for proteasome nuclear localization revealed by the structure of the nuclear proteasome tether protein Cut8. *Proc. Natl. Acad. Sci. U.S.A.* 108, 16950–16955.
- (13) Zhang, F., Su, K., Yang, X., Bowe, D. B., Paterson, A. J., and Kudlow, J. E. (2003) O-GlcNAc modification is an endogenous inhibitor of the proteasome. *Cell* 115, 715–725.
- (14) Zhang, F., Hu, Y., Huang, P., Toleman, C. A., Paterson, A. J., and Kudlow, J. E. (2007) Proteasome function is regulated by cyclic AMP-dependent protein kinase through phosphorylation of Rpt6. *J. Biol. Chem.* 282, 22460–22471.
- (15) Satoh, K., Sasajima, H., Nyomura, K. I., Yokosawa, H., and Sawada, H. (2001) Assembly of the 26S proteasome is regulated by phosphorylation of the p45/Rpt6 ATPase subunit. *Biochemistry* 40, 314–319.

- (16) Bose, S., Stratford, F. L., Broadfoot, K. I., Mason, G. G., and Rivett, A. J. (2004) Phosphorylation of 20S proteasome  $\alpha$  subunit C8 ( $\alpha 7$ ) stabilizes the 26S proteasome and plays a role in the regulation of proteasome complexes by  $\gamma$ -interferon. *Biochem. J.* 378, 177–184.
- (17) Iwafune, Y., Kawasaki, H., and Hirano, H. (2004) Identification of three phosphorylation sites in the  $\alpha 7$  subunit of the yeast 20S proteasome in vivo using mass spectrometry. *Arch. Biochem. Biophys.* 431, 9–15.
- (18) Kikuchi, J., Iwafune, Y., Akiyama, T., Okayama, A., Nakamura, H., Arakawa, N., Kimura, Y., and Hirano, H. (2010) Co- and post-translational modifications of the 26S proteasome in yeast. *Proteomics* 10, 2769–2779.
- (19) Kimura, Y., Saeki, Y., Yokosawa, H., Polevoda, B., Sherman, F., and Hirano, H. (2003) N-Terminal modifications of the 19S regulatory particle subunits of the yeast proteasome. *Arch. Biochem. Biophys.* 409, 341–348.
- (20) Kimura, Y., Takaoka, M., Tanaka, S., Sassa, H., Tanaka, K., Polevoda, B., Sherman, F., and Hirano, H. (2000) N( $\alpha$ )-acetylation and proteolytic activity of the yeast 20S proteasome. *J. Biol. Chem.* 275, 4635–4639.
- (21) Wang, X., Chen, C. F., Baker, P. R., Chen, P. L., Kaiser, P., and Huang, L. (2007) Mass spectrometric characterization of the affinity-purified human 26S proteasome complex. *Biochemistry* 46, 3553–3565.
- (22) Gomes, A. V., Zong, C., Edmondson, R. D., Li, X., Stefani, E., Zhang, J., Jones, R. C., Thypambil, S., Wang, G. W., Qiao, X., Bardag-Gorce, F., and Ping, P. (2006) Mapping the murine cardiac 26S proteasome complexes. *Circ. Res.* 99, 362–371.
- (23) Shibahara, T., Kawasaki, H., and Hirano, H. (2002) Identification of the 19S regulatory particle subunits from the rice 26S proteasome. *Eur. J. Biochem.* 269, 1474–1483.
- (24) Resh, M. D. (1999) Fatty acylation of proteins: New insights into membrane targeting of myristoylated and palmitoylated proteins. *Biochim. Biophys. Acta* 1451, 1–16.
- (25) Lander, G. C., Estrin, E., Matyskiela, M. E., Bashore, C., Nogales, E., and Martin, A. (2012) Complete subunit architecture of the proteasome regulatory particle. *Nature* 482, 186–191.
- (26) Baudin, A., Ozier-Kalogeropoulos, O., Denouel, A., Lacroute, F., and Cullin, C. (1993) A simple and efficient method for direct gene deletion in *Saccharomyces cerevisiae*. *Nucleic Acids Res.* 21, 3329–3330.
- (27) Longtine, M. S., McKenzie, A., III, Demarini, D. J., Shah, N. G., Wach, A., Brachat, A., Philippsen, P., and Pringle, J. R. (1998) Additional modules for versatile and economical PCR-based gene deletion and modification in *Saccharomyces cerevisiae*. *Yeast* 14, 953–961.
- (28) Sikorski, R. S., and Hieter, P. (1989) A system of shuttle vectors and yeast host strains designed for efficient manipulation of DNA in *Saccharomyces cerevisiae*. *Genetics* 122, 19–27.
- (29) Leggett, D. S., Glickman, M. H., and Finley, D. (2005) Purification of proteasomes, proteasome subcomplexes, and proteasome-associated proteins from budding yeast. *Methods Mol. Biol.* 301, 57–70.
- (30) Smith, D. M., Chang, S. C., Park, S., Finley, D., Cheng, Y., and Goldberg, A. L. (2007) Docking of the proteasomal ATPases' carboxyl termini in the 20S proteasome's  $\alpha$  ring opens the gate for substrate entry. *Mol. Cell* 27, 731–744.
- (31) Cabrera, R., Sha, Z., Vadakkan, T. J., Otero, J., Kriegenburg, F., Hartmann-Petersen, R., Dickinson, M. E., and Chang, E. C. (2010) Proteasome nuclear import mediated by Arc3 can influence efficient DNA damage repair and mitosis in *Schizosaccharomyces pombe*. *Mol. Biol. Cell* 21, 3125–3136.
- (32) Qian, S. B., Ott, D. E., Schubert, U., Bennink, J. R., and Yewdell, J. W. (2002) Fusion proteins with COOH-terminal ubiquitin are stable and maintain dual functionality in vivo. *J. Biol. Chem.* 277, 38818–38826.
- (33) Prufert, K., Alsheimer, M., Benavente, R., and Krohne, G. (2005) The myristoylation site of meiotic lamin C2 promotes local nuclear membrane growth and the formation of intranuclear membranes in somatic cultured cells. *Eur. J. Cell Biol.* 84, 637–646.
- (34) Zhang, F., Hu, M., Tian, G., Zhang, P., Finley, D., Jeffrey, P. D., and Shi, Y. (2009) Structural insights into the regulatory particle of the proteasome from *Methanocaldococcus jannaschii*. *Mol. Cell* 34, 473–484.
- (35) Chen, L., Romero, L., Chuang, S. M., Tournier, V., Joshi, K. K., Lee, J. A., Kovvali, G., and Madura, K. (2011) Sts1 plays a key role in targeting proteasomes to the nucleus. *J. Biol. Chem.* 286, 3104–3118.
- (36) Ashrafi, K., Farazi, T. A., and Gordon, J. I. (1998) A role for *Saccharomyces cerevisiae* fatty acid activation protein 4 in regulating protein N-myristoylation during entry into stationary phase. *J. Biol. Chem.* 273, 25864–25874.
- (37) Tanaka, K., and Ichihara, A. (1989) Half-life of proteasomes (multiprotease complexes) in rat liver. *Biochem. Biophys. Res. Commun.* 159, 1309–1315.
- (38) Chai, Y., Koppenhafer, S. L., Shoesmith, S. J., Perez, M. K., and Paulson, H. L. (1999) Evidence for proteasome involvement in polyglutamine disease: Localization to nuclear inclusions in SCA3/MJD and suppression of polyglutamine aggregation in vitro. *Hum. Mol. Genet.* 8, 673–682.